J|A|C|S
ARTICLES
Published on Web 04/07/2005

$Ag_4V_2O_6F_2$: An Electrochemically Active and High Silver Density Phase

Erin M. Sorensen,[†] Heather K. Izumi,[†] John T. Vaughey,[‡] Charlotte L. Stern,[†] and Kenneth R. Poeppelmeier*,[†]

Contribution from the Department of Chemistry, Northwestern University, Evanston, Illinois 60208-3113, and Chemical Engineering Division, Argonne National Laboratory, Illinois 87185-0755

Received January 10, 2005; E-mail: krp@northwestern.edu

Abstract: Low-temperature hydrothermal techniques were used to synthesize single crystals of $Ag_4V_2O_6F_2$. This previously unreported oxide fluoride phase was characterized by single-crystal X-ray diffraction and IR spectroscopy and was also evaluated as a primary lithium battery cathode. Crystal data: monoclinic, space group $P2_1/n$ (No. 14), with $a = 8.4034(4)$ Å, $b = 10.548(1)$ Å, $c = 12.459(1)$ Å, $\beta = 90.314(2)°$, and $Z = 4$. $Ag_4V_2O_6F_2$ (SVOF) exhibits two characteristic regions within the discharge curve, an upper plateau at 3.5 V, and a lower sloped region around 2.3 V from reduction of the vanadium oxide fluoride framework. The material has a nominal capacity of 251 mAh/g, with 148 mAh/g above 3 V. The upper discharge plateau at 3.5 V is nearly 300 mV over the silver reduction potential of the commercial primary battery material, $Ag_2V_4O_{11}$ (SVO).

Introduction

Vanadium oxides have long been studied as potential battery materials for primary or secondary lithium battery applications.[1] They have several intrinsic advantages such as large capacity, high voltage, and, owing to their layered nature, excellent kinetics that make them attractive battery materials. Their major drawback, however, is the tendency of vanadium oxides to become amorphous upon cycling, which limits their utility. Numerous studies have shown that adding a second metal cation to the structure, i.e., LiV_3O_8, $Ag_2V_4O_{11}$, or MnV_2O_5, can increase the framework stability upon lithium insertion.[2−6] $Ag_2V_4O_{11}$, or silver vanadium oxide (SVO), has been well characterized and is used commercially as a cathode material in primary lithium batteries for high-rate applications, such as those used in implantable cardioverter defibrillators (ICDs).[7−9] An ICD monitors the heartbeat and, when arrhythmia is detected, interrupts the fibrillation by delivering a shock of 30−35 J to the heart to restore normal rhythm. To deliver the shock, capacitors are rapidly charged to a high voltage and then discharged directly into the heart via electrical leads.[10] As a result, the battery requirements are very exacting and include delivering not only high capacity for long device life but also high voltage and power to recharge capacitors quickly.[11]

A long-term goal of the medical battery industry is to increase the capacity of the cathode above 3 V, while maintaining high electrode stability. To achieve this, alternative compounds are constantly under evaluation. In SVO, the initial voltage plateau at 3.25 V corresponds to silver reduction. A secondary plateau, corresponding to vanadium reduction, occurs at roughly 2.5 V. While SVO has a high capacity (315 mAh/g), 71% of the capacity is a result of V^{5+}/V^{4+} reduction. Further reduction of V^{4+} to V^{3+} occurs at voltages too low for use in an ICD.[12−16] A silver vanadate with a greater Ag:V molar ratio would increase the high-voltage component of the electrode; however, the silver vanadates with a Ag:V ratio greater than 1:2 tend to have very poor kinetics, low usable capacity, or low conductivity.[7]

An alternative approach to incorporating a higher Ag:V ratio in a mixed metal oxide is to replace oxide with more electronegative fluoride anions. A high mole fraction AgF phase could increase the silver content without completely eliminating the dimensionality of the vanadium oxide framework, thus maintaining some conduction pathways between vanadium centers while increasing the reduction potential of the material. Hy-

[†] Northwestern University.
[‡] Argonne National Laboratory.

(1) Whittingham, M. S. *Chem. Rev. (Washington, DC)* **2004**, *104*, 4271−4301.
(2) Zhang, F.; Whittingham, M. S. *Electrochem. Commun.* **2000**, *2*, 69−71.
(3) Selvaggi, A.; Croce, F.; Scrosati, B. *J. Power Sources* **1990**, *32*, 389−396.
(4) Scrosati, B.; Selvaggi, A.; Croce, F.; Wang, G. *J. Power Sources* **1988**, *24*, 287−294.
(5) Nassau, K.; Murphy, D. W. *J. Non-Cryst. Solids* **1981**, *44*, 297−304.
(6) Garcia-Alvarado, F.; Tarascon, J. M. *Solid State Ionics* **1994**, *73*, 247−254.
(7) Takeuchi, K. J.; Marschilok, A. C.; Davis, S. M.; Leising, R. A.; Takeuchi, E. S. *Coord. Chem. Rev.* **2001**, *219*, 283−310.
(8) Liang, C. C.; Bolster, M. E.; Murphy, R. M. US Patent 4,391,729, July 5, 1983.
(9) Liang, C. C.; Bolster, M. E.; Murphy, R. M. US Patent 4,310,609, January 12, 1982.
(10) Schmidt, C.; Tam, G.; Scott, E.; Norton, J.; Chen, K. *J. Power Sources* **2003**, *119−121*, 979−985.
(11) Takeuchi, E. S. *J. Power Sources* **1995**, *54*, 115−119.
(12) Takeuchi, E. S.; Thiebolt, W. C. *J. Electrochem. Soc.* **1988**, *135*, C343−C343.
(13) Takeuchi, E. S.; Quattrini, P. J.; Greatbatch, W. *PACE* **1988**, *11*, 2035−2039.
(14) Takeuchi, E. S.; Thiebolt, W. C. *J. Electrochem. Soc.* **1988**, *135*, 2691−2694.
(15) Leising, R. A.; Takeuchi, E. S. *Chem. Mater.* **1993**, *5*, 738−742.
(16) Crespi, A. M. US Patent 5,221,453, June 22, 1993.

drothermal synthetic techniques have been used extensively to obtain new phases that are inaccessible using high-temperature solid state techniques. Mixed metal oxide fluorides have been shown to readily form under mild hydrothermal conditions from their respective oxides and hydrofluoric acid; the hydrofluoric acid serves as both a fluoride source and a mineralizer.[17−19] Single crystals of $Ag_4V_2O_6F_2$, which is the first phase reported in the $Ag_2O{\cdot}V_2O_5{\cdot}AgF$ system, have been hydrothermally synthesized from Ag_2O, V_2O_5, and aqueous hydrofluoric acid. The crystal structure determination reveals a compound with sheets of vanadium oxide fluoride chains separated by silver cations. The synthesis and structural characterization of $Ag_4V_2O_6F_2$, as well as its electrochemical performance, are discussed below.

Experimental Section

Caution. Hydrofluoric acid is toxic and corrosive and must be handled with extreme caution and the appropriate protective gear! If contact with the liquid or vapor occurs, proper treatment procedures should immediately be followed.[20−22]

Materials. $Ag_4V_2O_6F_2$ was synthesized by sealing 0.4639 g (2.002×10^{-3} mol) of Ag_2O, 0.0911 g (5.009×10^{-4} mol) of V_2O_5, and 0.3036 g (1.517×10^{-2} mol) of aqueous HF in a Teflon (fluoroethylenepropylene) pouch.[23] The pouch was placed in a 250 mL Parr autoclave filled 33% with deionized H_2O as backfill, with up to six other pouches of varied composition. The autoclave was heated for 24 h at 150 °C and cooled to room temperature over an additional 24 h. The pouch was opened in air, and the products were recovered by vacuum filtration.

Crystallographic Determination. Single-crystal X-ray diffraction data were collected with Mo Kα radiation ($\lambda = 0.71073$ Å) on a Bruker SMART-1000 CCD diffractometer and integrated with the SAINT-Plus program.[24] The structure was solved by direct methods and refined using full-matrix least-squares techniques.[25] The crystal was twinned, and consequently the structure was refined using a twin refinement (β was close to 90°, which emulates orthorhombic symmetry). A face indexed absorption correction was applied using the program XPREP. The structure was checked for missing symmetry elements with PLATON.[26] The final refinement includes anisotropic displacement parameters for all atoms. See Figure 1 for a thermal ellipsoid plot, Table 1 for crystallographic data, and Supporting Information for the X-ray crystallographic file.

Spectroscopic Measurements. A mid-infrared (400−4000 cm^{-1}) spectrum was collected using a Bio-Rad FTS-60 FTIR spectrometer operating at 2 cm^{-1} resolution.

Electrochemical Characterization. Crystals of $Ag_4V_2O_6F_2$ were finely ground and then mixed with 10 wt % acetylene black and 10 wt % polyvinylidenedifluoride (PvDF) binder. The electrode mixture was then laminated onto aluminum foil and dried at 75 °C for 1 h in air before use. Electrochemical cells were constructed in an argon-filled glovebox using lithium as the negative electrode. The electrodes were separated by a Celgard separator, and a 1 M $LiPF_6$ in a 1:1 by weight mixture of ethylene carbonate (EC)/diethyl carbonate (DEC) solution was used as the electrolyte. Cells were discharged using either a 0.001 mA constant current to 0.75 V cutoff on a MacPile II galvanostat/potentiostat or by stepping in 0.05 V increments using a 0.1 mA current with 6 h rests between voltage steps to 1.75 V cutoff on a Maccor galvanostat.

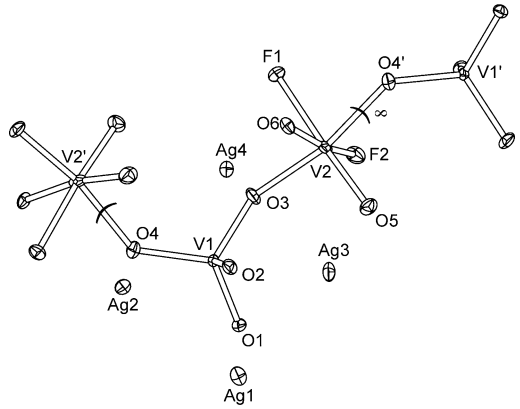

Figure 1. Thermal ellipsoid plot (showing 50% probability) of $Ag_4V_2O_6F_2$.

Table 1. Crystallographic Data for $Ag_4V_2O_6F_2$

formula	$Ag_4V_2O_6F_2$
fw	667.36
space group	$P2_1/n$ (No. 14)
a (Å)	5.594(1)
b (Å)	10.548(1)
c (Å)	12.459(1)
β (deg)	90.314(2)
V (Å^3)	735.2(1)
Z	4
T (°C)	−120(1)
λ (Å)	0.71069
ρ_{calc} (g/cm^3)	6.030
μ (mm^{-1})	12.916
$R(F)^a$	0.0342
$wR_2(F^2)^b$	0.0776

$^a R = \sum||F_o| - |F_c||/\sum|F_o|$. $^b wR_2 = [\sum w(F_o^2 - F_c^2)^2/\sum w(F_o^2)^2]^{1/2}$.

Results

Synthesis. The reported synthesis has been optimized through a number of reactions that varied the reactant ratio of Ag_2O:V_2O_5:HF(aq). Based on the formula stoichiometry, a minimum molar ratio of 2:1 Ag_2O to V_2O_5 was used. For reactions of 2:1 Ag_2O to V_2O_5, the aqueous HF was added in a molar ratio of approximately 2:1:7 up to 2:1:35. While crystals of $Ag_4V_2O_6F_2$ formed for all conditions, unreacted V_2O_5 was also present. Additional reactions that varied the metal oxide ratios were performed from 2:1 up to 4:1 Ag_2O to V_2O_5. The reported synthesis has a ratio of 4:1:30 Ag_2O:V_2O_5:HF(aq) and produces orange-red needles of $Ag_4V_2O_6F_2$ as the sole product in approximately 95% yield based on V_2O_5.[27]

Structure. The structure of $Ag_4V_2O_6F_2$ is made up of sheets of chains that align parallel to the *ab*-plane. Each chain is comprised of alternating V^{5+} centered tetrahedra and octahedra that are corner-shared to form undulating chains. See Figure 2.

V1 is tetrahedrally coordinated to four oxide ligands: two terminal oxides at short distances of V1−O1 = 1.695(6) Å and V1−O2 = 1.717(7) Å, and two bridging oxides at slightly longer distances of V1−O3 = 1.759(6) Å and V1−O4 = 1.753(6) Å to form $[VO_{2/2}O_2]^-$ units.

(17) Heier, K. R.; Norquist, A. J.; Wilson, C. G.; Stern, C. L.; Poeppelmeier, K. R. *Inorg. Chem.* **1998**, *37*, 76−80.
(18) Halasyamani, P.; Willis, M. J.; Stern, C. L.; Poeppelmeier, K. R. *Inorg. Chim. Acta* **1995**, *240*, 109−115.
(19) Maggard, P. A.; Nault, T. S.; Stern, C. L.; Poeppelmeier, K. R. *J. Solid State Chem.* **2003**, *175*, 27−33.
(20) Segal, E. B. *Chem. Health Saf.* **2000**, *7*, 18−23.
(21) Peters, D.; Miethchen, R. *J. Fluorine Chem.* **1996**, *79*, 161−165.
(22) Bertolini, J. C. *J. Emerg. Med.* **1992**, *10*, 163−168.
(23) Harrison, W. T. A.; Nenoff, T. M.; Gier, T. E.; Stucky, G. D. *Inorg. Chem.* **1993**, *32*, 2437−2441.
(24) *SAINT-Plus*, version 6.02A; Bruker Analytical X-ray Instruments, Inc.: Madison, WI.
(25) Sheldrick, G. M. *SHELXTL*, version 5.10; Bruker Analytical X-ray Instruments, Inc.: Madison, WI.
(26) Spek, A. L. PLATON, Utrecht University: Utrecht, The Netherlands.
(27) Izumi, H. K.; Sorensen, E. M.; Vaughey, J. T.; Poeppelmeier, K. R. US Provisional Patent 60/606,475, September 1, 2004.

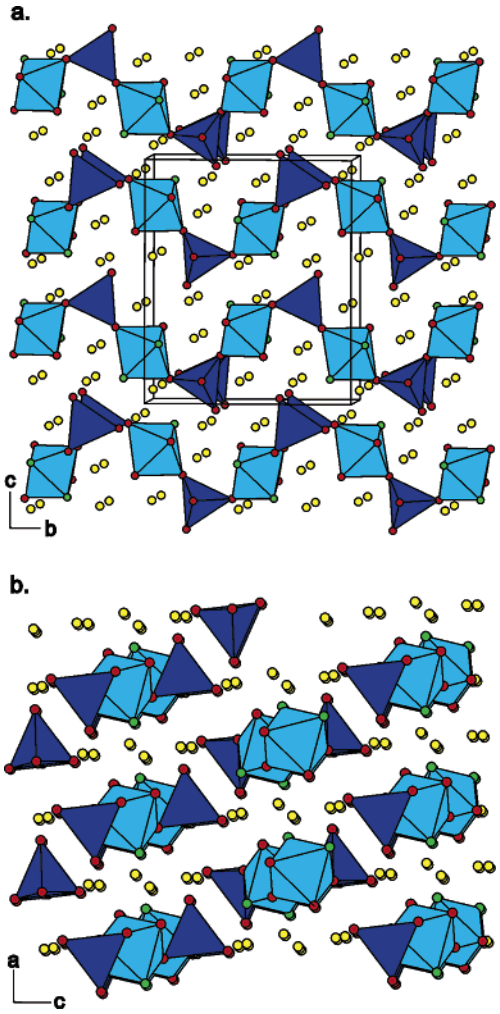

Figure 2. Three-dimensional packing diagrams of $Ag_4V_2O_6F_2$. (a) Chains of alternating vanadium oxide tetrahedra and vanadium oxide fluoride octahedra separated by silver ions. (b) Sheets formed by vanadium oxide fluoride chains separated by silver ions. Yellow spheres represent silver atoms, vanadium oxide fluoride octahedra are light blue, and vanadium oxide tetrahedra are dark blue.

In contrast, V2 is octahedrally coordinated to two terminal oxides, two fluorides that are *trans* to the terminal oxides, and two bridging oxides to give $[VO_{2/2}O_2F_2]^{3-}$. Like other oxide fluoride anions of the early d^0 transition metals, $[VO_{2/2}O_2F_2]^{3-}$ is found in a distorted octahedral environment.[17,28,29] The vanadium cation (V^{5+}) moves from the center of its octahedron toward the edge shared by the two terminal oxides to form short, strong bonds[30] at V2−O5 = 1.666(6) Å and V2−O6 = 1.739(6) Å, while the fluorides *trans* to the terminal oxides form longer, weak bonds at V2−F1 = 2.077(5) Å and V2−F2 = 1.945(6) Å. The bridging oxides, O3 and O4, are at distances of 1.958(6) and 1.979(6) Å from V2, respectively.

The IR spectrum shows four bands at 963, 922, 893, and 856 cm^{-1} in the metal−oxygen double bond fingerprint region (800−1000 cm^{-1}) of the spectrum. The bands at 963 and 893 cm^{-1} are assigned to the symmetric and asymmetric VO_2 (terminal) stretches of the VO_4F_2 octahedron, respectively. The

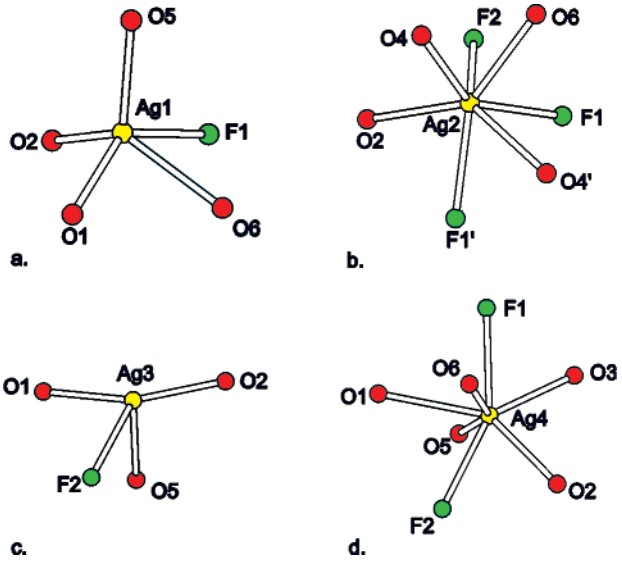

Figure 3. Coordination environment of silver atoms in $Ag_4V_2O_6F_2$. (a) Distorted square pyramidal, Ag1. (b) Distorted capped trigonal prismatic, Ag2. (c) Irregular sawhorse, Ag3. (d) Distorted pentagonal bicapped pyramidal, Ag4. Yellow spheres represent silver atoms, red spheres represent oxygen atoms, and green spheres represent fluorine atoms.

symmetric and asymmetric VO_2(terminal) stretches of the VO_4 tetrahedron are assigned to the bands at 922 and 856 cm^{-1}. The broad envelope centered around 720 cm^{-1} is attributed to stretches of the VO_4 tetrahedron.[31,32]

The silver ions sit in pockets of negative charge between the sheets of negatively charged vanadium oxide fluoride chains, which leads to irregular coordination environments. At a maximum coordination distance of 2.7 Å,[33] Ag1 is five-coordinate, Ag3 is four-coordinate, and both Ag2 and Ag4 are seven-coordinate. The different coordination environments around the silver cation create four crystallographically unique silver sites.

Ag1 has distorted square pyramidal coordination, with O5 at the apex and O1, O2, O6, and F1 forming the base. The Ag2 coordination forms a distorted capped trigonal prism geometry. The two triangular faces are made up of O4 × 2, F1 × 2, and F2. One of the rectangular faces of the prism is capped by O6. Ag3 is coordinated in an irregular sawhorse fashion to O1, O2, O5, and F2. Ag4 is coordinated in a distorted pentagonal bicapped pyramid geometry. O5 and O6 form apical bonds to Ag4, and O1, O2, O3, and F1 × 2 coordinated equatorially. See Figure 3.

Discussion

Primary lithium batteries are used for implantable medical devices because they typically offer higher capacity, reliability, and rate capability compared to secondary lithium batteries. For medical devices, various types of batteries are used depending upon the current rate required. Li/I_2, Li/CF_x, and $Li/Ag_2V_4O_{11}$ are used for low-, mid-, and high-rate systems, respectively.[34−38]

(28) Welk, M. E.; Norquist, A. J.; Stern, C. L.; Poeppelmeier, K. R. *Inorg. Chem.* **2000**, *39*, 3946−3947.
(29) Welk, M. E.; Norquist, A. J.; Stern, C. L.; Poeppelmeier, K. R. *Inorg. Chem.* **2001**, *40*, 5479−5480.
(30) Izumi, H. K.; Kirsch, J. E.; Stern, C. L.; Poeppelmeier, K. R. *Inorg. Chem.* **2005**, *44*, 884−895.
(31) Kristallov, L. V.; Volkov, V. L.; Perelyaeva, L. A. *Russ. J. Inorg. Chem.* **1990**, *35*, 1031−1034.
(32) Kristallov, L. V.; Volkov, V. L.; Perelyaeva, L. A. *Zh. Neorg. Khim.* **1990**, *35*, 1810−1814.
(33) Swarnabala, G.; Rajasekharan, M. V. *Polyhedron* **1996**, *16*, 921−925.
(34) Drews, J.; Fehrmann, G.; Staub, R.; Wolf, R. *J. Power Sources* **2001**, *97*−*98*, 747−749.
(35) Takeuchi, E. S.; Leising, R. A. *MRS Bull.* **2002**, *27*, 624−627.
(36) Schmidt, C. L.; Skarstad, P. M. *J. Power Sources* **2001**, *97*−*8*, 742−746.

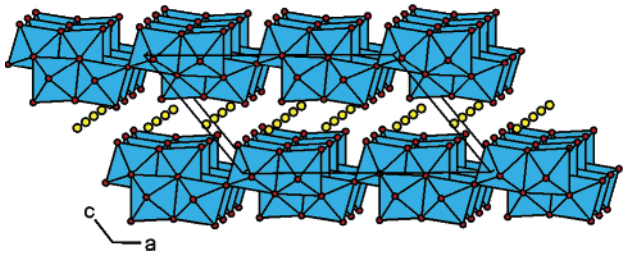

Figure 4. Three-dimensional packing diagram of $Ag_2V_4O_{11}$ (SVO) illustrating the layered nature of the structure. Yellow spheres represent silver atoms; vanadium oxide octahedra are blue.

$Ag_2V_4O_{11}$ (SVO) can insert up to 7 mol of lithium per mole of its formula unit at an initial open circuit voltage of 3.25 V, although battery design can further optimize the performance.[11,37,39] SVO is comprised of octahedrally coordinated vanadium oxide layers separated by silver ions. See Figure 4.[40]

One way to boost power would be to increase the average voltage of the active material. In the case of the silver vanadates, an increase in silver content could extend the time the potential is greater than 3 V. Silver pyrovanadate, $Ag_4V_2O_7$, has a Ag:V ratio greater than 1:2, making it seem a likely candidate; however, its structure is comprised of $[V_2O_7]^{4-}$ pyrovanadate anions with charge-balancing silver cations arranged in a hexagonally packed net. See Figure 5.[41] A thorough review of the literature does not result in any report of the electrochemical characterization of silver pyrovanadate. Because the material has discrete pyrovanadate anions, it is anticipated that its intrinsic conductivity would be low, and thus its ability to act as a high power cathode material would be hindered. Additionally, the tetrahedral coordination of the vanadium would make electrochemical reduction more difficult, since reduction would require an increase in the coordination sphere of the larger, reduced cation.[42]

Another route to increase the discharge voltage is to increase the electronegative character and number of the anionic ligands. In early work on lithium batteries, layered sulfides were the cathodes of choice, but the voltages of the sulfides were not sufficiently high for many applications. For this reason, the greater electronegativity of oxygen was exploited and, as expected, higher voltages were obtained with oxide phases.[43−45] Similarly, it has been calculated that $LiCaCoF_6$ would have an average intercalation voltage of 5.80 V versus 4.19 V observed experimentally in $LiCoO_2$.[46] Synthesizing oxide fluorides and fluorides, however, is not always straightforward, and thus few have been explored as electrode materials.[47−49] Hydrothermal techniques using the Teflon bag approach offer a low-temperature and self-contained method of synthesis.[23]

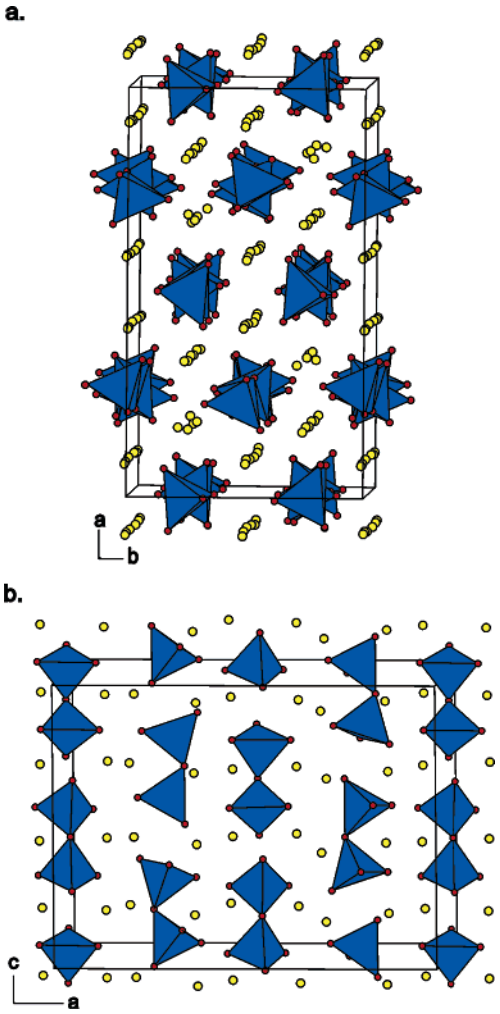

Figure 5. Three-dimensional packing of $Ag_4V_2O_7$. (a) Hexagonal packing of silver atoms and pyrovanadate units. (b) Discrete pyrovanadate units separated by silver atoms. Yellow spheres represent silver atoms; vanadium oxide tetrahedra are blue.

$Ag_4V_2O_6F_2$ (SVOF) has several properties that make it a potentially useful primary lithium battery material. SVOF has a higher silver-to-vanadium ratio than typical electrochemically active materials, while preserving critical connectivity in the vanadium oxide fluoride framework. Layered structures have long been desirable as electrode materials owing to their ability to maintain electrical contacts during lithium insertion and facilitate diffusion within the electrode.[45] In Figure 2, it can be seen that the silver ions lie between sheets of alternating vanadium tetrahedra and octahedra chains. This silver interlayer between the vanadium oxide fluoride sheets allows for lithium diffusion into the material and silver diffusion out of the material.

Two experiments were performed to determine the electrochemical properties of SVOF. In the first experiment, a low constant current was applied; the second open circuit voltage (OCV) experiment discharged the material by slowly stepping the voltage in 5 mV steps using a low current with 6 h rests between steps. For materials that require silver diffusion, e.g.,

(37) Crespi, A. M.; Somdahl, S. K.; Schmidt, C. L.; Skarstad, P. M. *J. Power Sources* **2001**, *96*, 33−38.
(38) Brodd, R. J.; Bullock, K. R.; Leising, R. A.; Middaugh, R. L.; Miller, J. R.; Takeuchi, E. S. *J. Electrochem. Soc.* **2004**, *151*, K1−K11.
(39) Takeuchi, E. S.; Keister, P. *J. Electrochem. Soc.* **1985**, *132*, C345−C345.
(40) Onoda, M.; Kanbe, K. *J. Phys.: Condens. Matter* **2001**, *13*, 6675−6685.
(41) Masse, R.; Averbuch-Pouchot, M. T.; Durif, A.; Guitel, J. C. *Acta Crystallogr., Sect. C: Cryst. Struct. Commun.* **1983**, *C39*, 1608−1610.
(42) Whittingham, M. S.; Zavalij, P. Y. *Int. J. Inorg. Mater.* **2001**, *3*, 1231−1236.
(43) Mizushima, K.; Jones, P. C.; Wiseman, P. J.; Goodenough, J. B. *Solid State Ionics* **1981**, *3*−*4*, 171−174.
(44) Mizushima, K.; Jones, P. C.; Wiseman, P. J.; Goodenough, J. B. *Mater. Res. Bull.* **1980**, *15*, 783−789.
(45) Whittingham, M. S. In *Lithium Ion Batteries, Fundamentals and Performance*; Wakihara, M., Yamamoto, O., Eds.; Wiley-VCH: New York, 1998; pp 49−66.
(46) Koyama, Y.; Tanaka, I.; Adachi, H. *J. Electrochem. Soc.* **2000**, *147*, 3633−3636.
(47) Fal'kengof, A. T.; Makhonina, E. V.; Zhigarnovskii, B. M.; Pervov, V. S.; Bogdanovskaya, V. A. *Izv. Akad. Nauk SSSR, Neorg. Mater.* **1990**, *26*, 2168−2171.
(48) Amatucci, G. G. 5,932,374, August 3, 1999.
(49) Amatucci, G. G. US Patent 5,759,720, June 2, 1998.

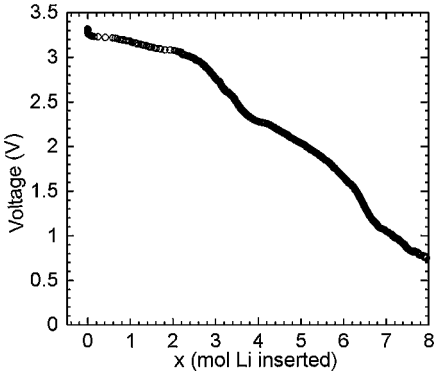

Figure 6. Constant current discharge curve of $Ag_4V_2O_6F_2$.

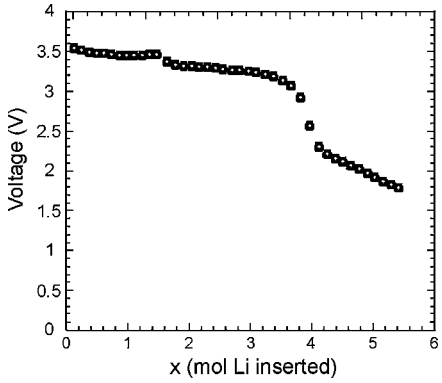

Figure 7. Open circuit voltage curve of $Ag_4V_2O_6F_2$.

SVO and most likely SVOF, the measured potentials at higher rates are frequently depressed, since the voltage of a battery is the potential measured at the electrode surface. As the current is applied, current flow is limited by the diffusion of lithium into the structure and, in this case, diffusion of silver out of the structure. The electrode surface is thus more reduced than the electrode bulk, and the potential across the cell drops. When the current is stopped, the lithium ions at the surface diffuse into the bulk and find their lowest energy position. The constant current experiment gives information about the total capacity of the material, and the OCV experiment clarifies the voltage plateaus of the electrode. Similar step voltage or pulse current experiments are used to characterize electrode materials such as SVOF as it helps separate the necessary cation diffusion steps from the true electrochemical performance.[16,50−52]

For devices that use high-rate batteries, e.g., ICDs, minimization of the volume and mass of the device is essential; thus, the cathode material must have high gravimetric and volumetric capacities. ICDs work most efficiently above 3 V, and therefore increasing the silver content in the ICD cathode would enhance the performance of the ICD. Complex engineered solutions to increase the capacity of SVO above 3 V have been used to some success;[37] however, a more straightforward chemical approach can be taken, as is the case with SVOF. SVO has a capacity of 315 mAh/g (1510 mAh/cm^3), equivalent to the insertion of 7 mol of lithium per formula unit, while SVOF has a capacity of 251 mAh/g (1513 mAh/cm^3) or 6.25 mol of lithium, with 1.5 V as the cutoff voltage.

The constant current discharge curve of voltage versus moles of lithium for SVOF is shown in Figure 6. Initially, there is a gentle slope at 3.25 V that extends until two lithium ions are inserted. The potential gradually decreases as additional lithium ions are inserted. The first region can be attributed to silver reduction. The slight slope of the upper discharge plateau is indicative of a single phase insertion, most likely associated with sluggish silver diffusion.[45] As the third and fourth lithium ions are inserted into the cathode, the voltage declines sharply, perhaps indicating that the structure may be transforming as the remaining silver is reduced and the lithium ions are inserted. The voltage continues to decrease in the second region of the plot, and the voltage decline is attributed to the reduction of V^{5+} to V^{4+}. Some of the capacity below 2 V can also be attributed to ethylene carbonate reduction; however, this is usually kinetically unfavorable and typically observed below 0.8 V. After the first vanadium reduction the potential falls below 1.5 V, which is less than the typical working voltages of most ICDs.

The OCV experiment shows the individual reduction events occurring within the electrode. As seen in the first experiment, there are two silver reduction events; the first plateau is at 3.52 V and the second is at 3.25 V. See Figure 7. The initial voltage plateau is nearly 300 mV higher than the silver reduction potential of SVO. It is apparent that the presence of the fluoride increases the reduction potential of the silver, as was suggested in the literature.[42,46,48,49] Looking at the silver coordination and Ag−O and Ag−F bonding, it is possible to speculate that Ag2 and Ag4, with three and two fluorides in their coordination sphere, respectively, reduce at a higher potential than the other two silver cations, which have only one fluoride ion in their coordination spheres. In addition to the higher reduction potential, the capacity of SVOF above 3 V is 148 mAh/g (892 mAh/cm^3), equivalent to 3.7 mol of lithium inserted, while SVO has a capacity of 100 mAh/g (480 mAh/cm^3).

Comparing the silver reduction regions of the OCV and the constant current experiments, it can be seen that the voltage in the OCV experiment is markedly higher than that of the constant current experiment. The voltage in the constant current experiment is lower owing to polarization within the electrode. The disparate voltages also indicate that the intrinsic conductivity of SVOF is most likely low; however, as silver metal plates onto the particles, the overall conductivity of the electrode increases. Polarization under constant current conditions is typical of electrodes requiring displacement reactions; thus OCV experiments are the primary means of characterizing these materials.

The vanadium reduction plateau in Figure 7 is slightly lower than would be expected; it is roughly 2 V rather than 2.5 V in SVO. In $Ag_4V_2O_6F_2$, the vanadium framework consists of chains formed by alternating vanadium oxide tetrahedra and vanadium oxide fluoride octahedra. In general, V^{5+} octahedra can be reduced without structural rearrangement, while V^{5+} tetrahedra cannot, because tetrahedral vanadium coordination exists only in the +5 oxidation state. Consequently, the presence of tetrahedra within the vanadium framework depresses the vanadium reduction potential and modifies the electrochemical behavior of SVOF.[42]

(50) Thiebolt, W. C.; Takeuchi, E. S. *J. Electrochem. Soc.* **1987**, *134*, C403−C403.
(51) Leising, R. A.; Thiebolt, W. C.; Takeuchi, E. S. *Inorg. Chem.* **1994**, *33*, 5733−5740.
(52) West, K.; Crespi, A. M. *J. Power Sources* **1995**, *54*, 334−337.

Conclusions

$Ag_4V_2O_6F_2$ is the first reported phase in the $Ag_2O{\cdot}V_2O_5{\cdot}AgF$ system. The incorporation of AgF increases the density of silver ions in the compound without eliminating the connectivity in the vanadium oxide fluoride framework. Owing to the high mole fraction of silver, SVOF has a higher capacity above 3 V of 148 mAh/g, in comparison to 100 mAh/g in SVO. In addition to the increased capacity, the silver reduction potential of SVOF is 3.52 V, 300 mV higher than that of SVO, which is due to fluoride incorporation.

Acknowledgment. The authors gratefully acknowledge the support from the National Science Foundation (Solid State Chemistry Award No. DMR-9727516 and DMR-0312136), the Office of Naval Research (MURI Grant N00014-01-1-0810), the Department of Energy's Office of Science, and the use of the Central Facilities supported by the MRSEC program of the National Science Foundation (DMR-0076097) at the Materials Research Center of Northwestern University.

Supporting Information Available: An X-ray crystallographic file in CIF format including crystallographic details, atomic coordinates, anisotropic thermal parameters, interatomic distances and angles, and the infrared spectrum of $Ag_4V_2O_6F_2$. This material is available free of charge via the Internet at http://pubs.acs.org.

JA050150F